

Inhibition of LaNi₅ electrode decay in alkaline medium by electroless encapsulation of active powder particles

M. Dymek¹ · H. Bala¹

Received: 6 March 2016 / Revised: 27 March 2016 / Accepted: 30 March 2016 / Published online: 12 April 2016
© The Author(s) 2016. This article is published with open access at Springerlink.com

Abstract Surface of powdered LaNi₅ intermetallic compound has been modified by active particle coverage with electroless nickel (Ni-P). The electrode degradation process in 6 M KOH solution has been tested across 70 charge/discharge cycles at $-0.5\text{ C}/+0.5\text{ C}$ rates. It has been established that after approx. 25–35 initial cycles, the electrode degradation process fulfills first order chemical reaction kinetics law: logarithm of discharge capacity linearly decreases with cycle number. The rate constant for the Ni-P protected material is over 20 % lower than that of as received one. The surface modification also improves the alloy hydrogenation kinetics: exchange current densities of H₂O/H₂ system are generally greater for modified material and, contrary to uncovered material, do not practically decrease with long-lasting cycling.

Keywords Intermetallic compound · Hydride battery · Charge/discharge · Corrosion rate · Powder encapsulation · Ni-P coating

Introduction

One of the most important applications for alloys based on LaNi₅ intermetallic compound is their usefulness as the anodic materials for nickel metal hydride (NiMH) batteries [1–6].

Together with the NiOOH/Ni(OH)₂ counter electrode in strong alkaline solution, the LaNi₅-type electrode materials (usually Ni is partly substituted by such elements as Co, Al, Mn, Fe, etc.) form very efficient and heavy duty battery systems with EMF equal to 1.2 V, often resistant to more than 1000 charge/discharge cycles. Commercialization of the NiMH type systems started with small cylindrical cells (700 to 5000 mA h) for portable electronic devices and progressed to large, 100 A h cells for hybrid electric vehicles and stationary applications [1]. It needs to be emphasized that the NiMH type batteries have ventured into the market with advantages in high capacity, good electrochemical catalysis, long service life, a wide temperature range, low costs averaged over the service life, and environmental compatibility [1, 4–7].

The resistance of LaNi₅ based materials to degradation processes in alkaline media is limited mainly because of high electrochemical activity of lanthanum (and other rare-earth elements). Owing to effective lanthanum passivation in strong alkaline media, the corrosion behavior of LaNi₅ based alloys is generally satisfactory; however, there are big literature differences in corrosion rates between LaNi₅ based alloys containing various substitutions or additions. The reasons and mechanisms of corrosion of hydride materials containing rare earth elements in view of worsening of their electrochemical parameters were subject of many publications, e.g., Refs [8–15].

It is worth noting that efficient hydrogen absorption of a number of intermetallics (including LaNi₅ type alloys) is possible when these alloys are powdered to form particles of dimensions of some μm . The crystal lattice expansion/contraction occurring during hydride material cycling (charging and discharging) is prone to further particle cracking, pulverization, and other forms of degradation, always accompanied with oxidation of alloy constituents. The oxidation processes of La and Ni in alkaline solutions occur rather slowly, owing to passivation. Nevertheless, it is impossible to

✉ M. Dymek
mdymek@wip.pcz.pl

H. Bala
hbala@wip.pcz.pl

¹ Department of Chemistry, Czestochowa University of Technology, al. Armii Krajowej 19, 42-200 Czestochowa, Poland

determine massive hydride alloy corrosion rate on the basis of polarization measurements in alkaline media. Strictly speaking, the OCP potential of cathodically charged alloy read from potentiodynamic polarization curves in most of cases is close to -0.93 V (vs HgO/Hg), i.e., it corresponds to equilibrium potential of $\text{H}_2\text{O}/\text{H}_2$ system. This way, Tafel extrapolation method determines exchange current of $\text{H}_2\text{O}/\text{H}_2$ electrode but not corrosion current of the alloy [16]. In most of applications, hydride electrodes are prepared from powdered hydride materials, and it is rational to express both hydrogen exchange currents and alloy corrosion currents of such electrodes in mA/g.

Among studies under improvement of corrosion stability of powdered hydride electrodes, there appear papers dealing with protection of active particles by metallic coatings [9, 10, 17–22]. As the efficient coatings, the surface layers of such metals as Cu, Ni, Co, and Pd have been successfully applied. In one of our previous papers [22], we have shown that Ni-P electroless coatings satisfactorily inhibit degradation processes of composite, powdered $\text{LaNi}_{4.5}\text{Co}_{0.5}$ hydrogen storage electrode in strong alkaline solution. The encapsulation of $\text{LaNi}_{4.5}\text{Co}_{0.5}$ particles with $0.8\text{ }\mu\text{m}$ thick Ni-P layers gets longer electrode lifetime: its half capacity decay cycle number increases from 430 to 713 cycles [22]. Additionally, Ni-P coatings improve a little the charge/discharge kinetics for this Co-containing storage material [22]. In the cited paper, we have also shown that Ni-P encapsulation practically does not affect the starting discharge capacity of the active material. The latest observation is understandable, since capacity is a feature of the hydride alloy. However, this statement seems not to be obvious for alloys exhibiting hydrogen partial equilibrium pressure greater than the external pressure (i.e., $p_{\text{H}_2}^{\text{eq}} > 1$ bar). The increase of hydrogen pressure always favors hydrogen absorption [23]. As a consequence, full hydrogenation is possible for given hydride alloy when $p_{\text{H}_2}^{\text{eq}}$ for this alloy is lower than the H_2 external pressure. For $\text{LaNi}_{4.5}\text{Co}_{0.5}$ alloy, the $p_{\text{H}_2}^{\text{eq}}$ is 1.15 bar (22 °C) [24]; therefore, at atmospheric pressure (1.0 bar), one can expect nearly full saturation of this material with hydrogen (to obtain hydride stoichiometry close to $\text{LaNi}_{4.5}\text{Co}_{0.5}\text{H}_6$). On the other hand, for LaNi_5 compound $p_{\text{H}_2}^{\text{eq}}$ is noticeably greater: it equals 1.6 bar (20 °C) [25]. As result, the equilibrium solubility of atomic hydrogen in LaNi_5 is always comparatively low at ambient external pressures. In practice, when LaNi_5 cathodically charged at atmospheric conditions, it corresponds to stoichiometric index at H equal to approx. 2–3 [23, 26]. Even so, when the active particles are covered with tight seal, one should expect greater hydrogen pressure within porous particle inner structural discontinuities than the external pressure. Another words, one cannot exclude for materials of $p_{\text{H}_2}^{\text{eq}}$ significantly exceeding 1 bar, that tight encapsulation of material particles results in more efficient hydrogen absorption.

The present work aims at determining of the role of LaNi_5 particles encapsulation with electroless layers of Ni-P on electrochemical parameters characterizing the electrode hydrogenation properties as well as an effect of encapsulation on material degradation induced by long-lasting cycling in concentrated KOH solution. These results will act as reference data for our further attempts under surface modification of powders of commercial hydride materials.

Experimental procedure

High purity LaNi_5 intermetallic compound (Alfa Aesar GmbH, 99.9 %) has been used as the active electrode material. The alloy small pieces (4–6 mm) were powdered by milling (Fritsch, Pulverizette, Ar-atmosphere) and sieved to separate 20–50 μm fraction. The test electrodes have been prepared in two variants, using: (i) *as received* powder and (ii) powder modified with thin (ca 1 μm thick) layer of electroless nickel (particles encapsulated by Ni-P coatings). The protective Ni-P coatings have been formed by treatment of the sieved powder in the modification solution containing Ni(II) sulfate and sodium hypophosphite as reducing agent. The composition of the modification solution was as follows (in $[\text{g}\cdot\text{L}^{-1}]$): 25 $\text{NiSO}_4\cdot 7\text{H}_2\text{O}$, 25 NaH_2PO_2 , 10 CH_3COOH , pH = 5.9. The powder encapsulation was carried out during 5 min at moderate agitation and at a temperature of 80 °C, analogously as described in Ref. [19]. Such procedure ensured smooth, equithick amorphous Ni-based coatings on the LaNi_5 particles, enriched with 5 ± 2 mass % of phosphorus—see Fig. 1 [19].

The powders were thoroughly mixed with 5 mass % of C-graphite as a conductive powder and 10 mass % of poly(vinylidene fluoride)—PVDF as a particle binder. The composite electrodes were formed from the obtained mixtures by their pressing with a force of 5 MPa and had final form of pellets ($\phi = 5$ mm, $h \approx 0.3$ mm). The electrodes porosity, in terms of electrolyte accessibility to hydride material particles within the pellet, was approx. 7 vol.% [27] which ensured short time (25–30 min) of the pellet full soaking by the test solution. The mean mass of the pellet was $m_{\text{pellet}} = 0.0350$ g and it was being determined with the accuracy of ± 0.1 mg for each electrode. The share of active material in the pellet was 85.0 mass %; thus, the initial mass of the LaNi_5 powder in the test electrode was $m_{\text{M}} = 0.0298$ g, on average. The pellets were used as working electrodes in 30-mL teflon cell equipped with Au-auxiliary and HgO/Hg reference electrodes. The reference electrode was completed with Luggin's capillary to avoid ohmic potential drop in the solution. The charge/discharge measurements were carried out galvanostatically in deaerated (Ar saturated), 6 M KOH solution at 22 ± 0.2 °C, using CHI Instruments electrochemical station (Austin, Texas).

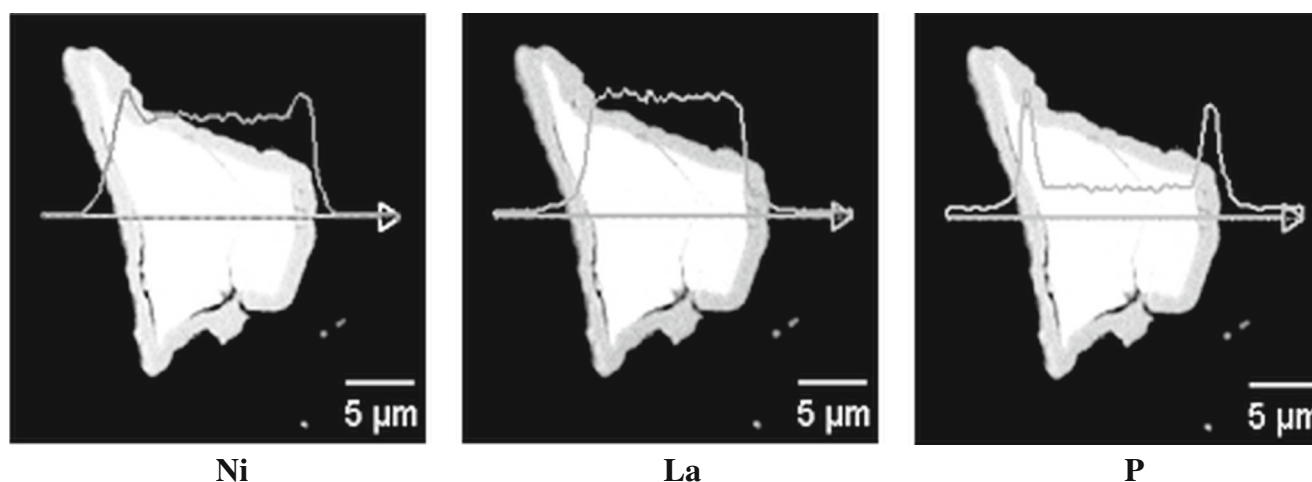


Fig. 1 Cross-section of the representative Ni-P encapsulated LaNi_5 particle and linear profiles of nickel, lanthanum, and phosphorus distribution (EDS microanalysis, Hitachi S-3400 N SEM microscope)

The rates of the charge and discharge processes were assumed to be -0.5 C and $+0.5\text{ C}$ (which corresponds to the external current densities of $|i_{0.5\text{ C}}| = 186\text{ mA g}^{-1}$). Owing to large ratio of electrolyte and pellet volumes, the temperature changes caused by electrode charge/discharge were negligible. The electrode charging has been assumed to be 9000 s for all cycles. The electrode charging/discharging has been carried out up to $N = 60\text{--}70$ cycles (for greater cycle numbers, the worsening of electrode coherence occurred, which was accompanied with partial losing of particles compact with binder).

All the electrode potentials were measured and are expressed vs HgO/Hg electrode. As the end potential for each cycle, the -0.50 V vs HgO/Hg has been set up. The time periods corresponding to the end potential have been considered as discharge times (t_{disch}).

The discharge capacity has been defined for given cycle as a product of discharge rate and discharge time ($Q_{\text{disch}} = 186 [\text{mA} \cdot \text{g}^{-1}] \times t_{\text{disch}} [\text{h}]$). The capacity changes vs cycle number have been presented in $\log Q_{\text{disch}} - N$ coordinate system because, as it has been proved in Ref. [22], the capacity fade of hydrogen absorbing alloys obeys first reaction order electrode material decay law:

$$\log Q_N = \log Q_0 - 0.434 k_{\text{degr}} N \quad (1)$$

¹ Q_N is expressed in mA h per 1.00 g of starting powdered hydrogen storage alloy in the pellet. Prior to contact with KOH solution, the material is not oxidized and its capacity takes on maximum value (Q_0). To measure such a value of capacity, the material needs to be activated. In case of LaNi_5 type alloys, full activation requires at least $5\text{--}10$ charge/discharge cycles. During electrode exploitation, the active particles undergo partial oxidation, structural destruction, etc., which is prone to gradual decrease of alloy active mass in the pellet. The electrode capacity is proportional to the actual amount of active material in the electrode pellet, m_M .

where Q_N denotes discharge capacity for given cycle number,¹ Q_0 is a maximum capacity corresponding to starting, non-oxidized storage material and 0.434 is reciprocal of $\ln 10$. The $k_{\text{degr}} [\text{cycle}^{-1}]$ denotes hydride material decay (degradation) rate constant (at given charge/discharge rate) and has a sense of first-order reaction kinetics rate constant. Substituting $Q_{N_{1/2}} = \frac{1}{2} Q_0$ into Eq. (1), we can define the so-called half capacity decay cycle number, $N_{1/2}$, that corresponds to the cycle number after which the electrode capacity falls to $Q_0/2$:

$$N_{1/2} = \frac{2.303 \log 2}{k_{\text{degr}}} = \frac{0.693}{k_{\text{degr}}} \quad (2)$$

The mass concentration of active hydride material in the electrode (c_M , $[\text{g} \cdot \text{cm}^{-3}]$) is defined for a given cycle as the actual mass of hydride alloy in the working composite pellet, m_M , per pellet volume.² The pellet density was 7.3 g cm^{-3} ; hence, starting mean pellet volume $V_0 = 0.0350\text{ g} / 7.3\text{ g cm}^{-3} = 0.0048\text{ cm}^3$ and starting concentration of active material $c_{M,0} = 0.0298\text{ g} / 0.0048\text{ cm}^3 = 6.2\text{ g cm}^{-3}$. The initial corrosion rate of the hydride electrode (corresponding to $N = 0$), expressed in $[\text{g} \cdot \text{cm}^{-3} \cdot \text{cycle}^{-1}]$, is:

$$r_{\text{corr},0} = k_{\text{degr}} c_{M,0} = k_{\text{degr}} \frac{m_{M,0}}{V_0} \approx 6.2 \cdot k_{\text{degr}} \quad (3)$$

The electrode corrosion rate (r_{corr}) decreases with electrode exploitation proceed because c_M concentration decreases with

² The working pellet is a complex, multicomponent system which contains 85.0 mass \% of active powder (LaNi_5), 5.0 mass \% of C-graphite, and 10.0 mass \% of PVDF (binder). Its porosity (in terms of electrolyte soaking) is about 7 vol\% (after 10 cycles) [27], so the pellet immersed in 6 M KOH solution increases its mass from 0.0350 g (dry pellet) to about 0.0354 g (fully soaked pellet). The hydride material mass concentration, c_M , must be treated as a formal quantity because the pellet uniformity is not on the molecular level. Finally, it must be taken into account that the charged pellet volume is a little greater than that of discharged one.

time (and, accordingly, with cycle number). For first order reaction, this decrease has exponential character: $c_M = c_{M,0}e^{-k_{\text{deg}}N}$. In particular, c_M falls twofold after $N_{1/2}$ cycle (compare Eq. (2)).

The exchange current densities of $\text{H}_2\text{O}/\text{H}_2$ system ($i_{\text{H}_2\text{O}/\text{H}_2}^0$) have been determined from charge/discharge plots, on the basis of potential jump (ΔE) that corresponds to the external current switching from negative (i_c) to positive (i_a) values, according to Refs [28–30]:

$$\log i_{\text{H}_2\text{O}/\text{H}_2}^0 = \frac{1}{2} \log(|i_c| \cdot i_a) - \frac{\Delta E}{2b} \quad (4)$$

In Eq. (4), b is the Tafel coefficient of cathodic and anodic straight lines of the hydrogen electrode, equal to 0.12 V on LaNi_5 type materials in strong alkaline solutions [16, 28]. Substituting charge and discharge rates to be in present study -186 and $+186 \text{ mA} \cdot \text{g}^{-1}$, respectively, the Eq. (4) takes on the following, numerical form:

$$\log i_{\text{H}_2\text{O}/\text{H}_2}^0 = 2.27 - \frac{\Delta E}{0.24} \quad (5)$$

The equations (1–5) have been employed to evaluate the fundamental electrochemical parameters of Ni-P encapsulated LaNi_5 , powder composite electrode. More details relating electrochemical measurement procedure applied in experimental part can be found in our previously published papers [19, 22–24, 29, 30].

Experimental results and discussion

In Fig. 2, representative plots of some chosen charge/discharge cycles are presented for the powdered composite LaNi_5 electrode in 6 M KOH solution. As it is seen, after a couple of first cycles, at $E > -0.7$ V, the anodic curves become practically vertical to the time axis which testifies to full discharge of the hydride electrode. Because of such nearly vertical plots, it is justified to read the discharge times (t_{disch}) for given cycle for the end potential ($E_{\text{end}} = -0.5$ V). The charge curves in Fig. 2 display step-like character which allows rough determining of the time periods corresponding to the nickel (II) oxide reduction, atomic hydrogen absorption, and hydrogen gas evolution, similarly as in Refs. [29, 30]. The reduction times enable determining of so-called reversible corrosion rates of Ni, as described in Refs [26, 29, 31]. The reversible corrosion of Ni is neglected in further discussion, since for long-lasting cycling the dominant for hydride material corrosion is the role of irreversible oxidation of lanthanum [22].

In Fig. 3, the long-lasting capacity fade is presented in $\log Q_{\text{disch}} - \text{cycle number}$ coordinate system for powder composite electrodes prepared from bare (full circles) and Ni-P encapsulated LaNi_5 particles (rectangles). It is seen that in

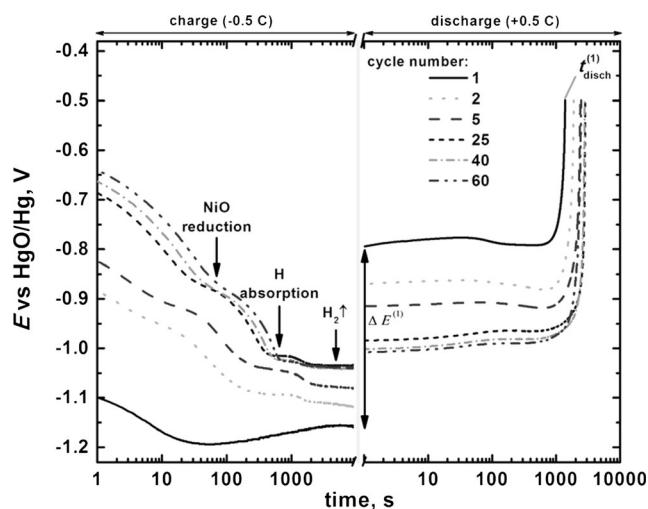


Fig. 2 Typical galvanostatic charge/discharge curves for uncoated LaNi_5 hydrogen storage material for chosen cycles. For charge curves, the regions responsible for Ni (II) oxide phase reduction, atomic hydrogen absorption, and H_2 -gas evolution are indicated by arrows. The ways of discharge time as well as potential jump (compare Eq.(4)) determining are visually shown on the example of $N = 1$ cycle. Experimental conditions: 6 M KOH solution, Ar, 22 °C, $-186/+186 \text{ mA g}^{-1}$, active material mass in the pellet: 0.0315 g, powder fraction: 20–50 μm

the beginning, the logarithm of capacity increases with cycling (up to $N \approx 20$) and after $N = 25$ –35 cycle, it starts to decrease linearly with further cycling. The continuous increase of the hydrogen capacity for initial cycles (up to $N \approx 30$ cycle) observed for both bare and encapsulated materials seems to testify for decisive role of hydride material activation, its surface development, and negligible effect of material oxidation in these cycles. The rectilinear segments satisfy the Eq.(1) with their slopes being -0.0028 and -0.0022 for bare and for encapsulated material, respectively. The experimental error corresponding to these slopes is very low; we evaluate it to be less than

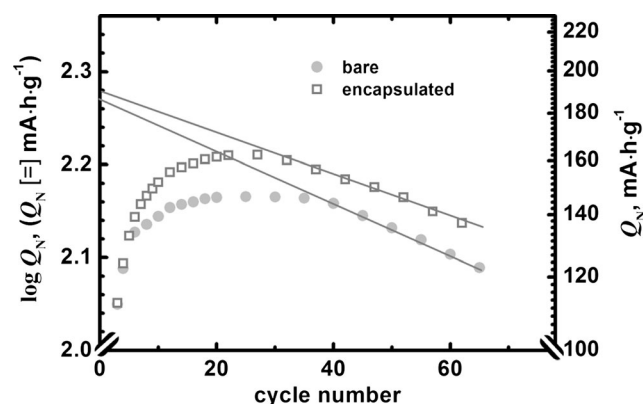


Fig. 3 Logarithm of discharge capacity as a function of cycling for LaNi_5 composite electrodes prepared from bare and Ni-P encapsulated powder particles. Initial corrosion rates found from slopes of the rectilinear segments are 0.040 and $0.033 \text{ g cm}^{-3} \text{ cycle}^{-1}$ for bare and Ni-P encapsulated material, respectively

± 1 %. These slopes testify to over 20 % lower electrode degradation rate for material encapsulated with Ni-P coating. The extrapolation of linear segments allows for determining of $\log Q_0$ for both electrodes (they are equal to 2.27 and 2.28 for bare and encapsulated powder, respectively). As seen, the Q_0 values are close to each other for both kinds of powder ($Q_{0,\text{bare}} = 10^{2.27} = 186 \text{ mA h g}^{-1}$ and $Q_{0,\text{encaps}} = 10^{2.28} = 190 \text{ mA h g}^{-1}$). Evidently, these values do not practically depend on powder encapsulation and are about 50 % less than the theoretical capacity of LaNi_5 ($Q_{\text{theor}} = 372 \text{ mA h g}^{-1}$ but it can be achieved when external pressure of H_2 exceeds $p_{\text{H}_2}^{\text{eq}} = 1.6 \text{ bar}$). It should be mentioned that for $\text{LaNi}_{4.5}\text{Co}_{0.5}$ hydrogen storage alloy, the Q_0 values were distinctly greater [22]: $255 \pm 4 \text{ mA h g}^{-1}$ (as it has been mentioned, $p_{\text{H}_2}^{\text{eq}}$ for $\text{LaNi}_{4.5}\text{Co}_{0.5}$ alloy is only slightly greater than 1 bar). These results rather exclude speculation that presence of Ni-P layers may be prone to noticeably greater hydrogen pressures inside of particles.

The degradation rate constants (k_{degr}) for LaNi_5 electrode, calculated from Eq. (1), are equal to: $6.5 \cdot 10^{-3}$ for bare and $5.0 \cdot 10^{-3} \text{ cycle}^{-1}$ for encapsulated powder. The rate constants for LaNi_5 compound read from data presented in Fig. 3 are 4–5 times greater than these found for Co substituted alloy [22] which confirms that partial substitution of Ni by Co is very advantageous from material corrosion resistance point of view. Accordingly, the calculated half capacity decay cycle numbers for LaNi_5 compound (Eq. 2) are $N_{1/2,\text{bare}} = 106$ and $N_{1/2,\text{encaps}} = 139$, i.e., are in similar proportions shorter (4 and 5 times, respectively) compared to those for $\text{LaNi}_{4.5}\text{Co}_{0.5}$ electrode [22]. Despite low corrosion resistance of LaNi_5 compound, it is seen that its encapsulation with protective Ni-P coating noticeably inhibits the active material degradation.

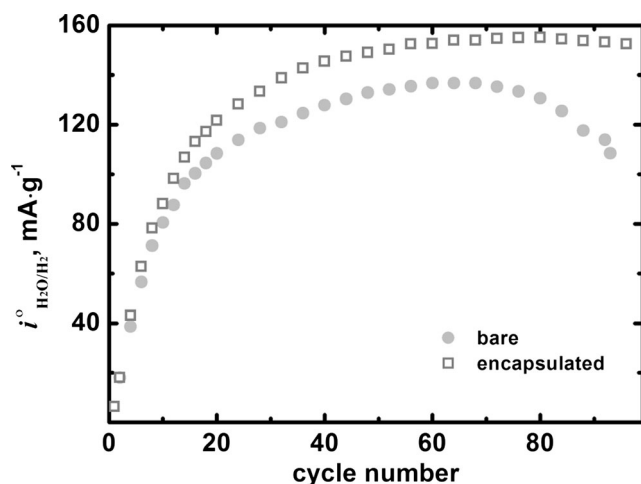


Fig. 4 Effect of cycling on exchange current density of $\text{H}_2\text{O}/\text{H}_2$ system for LaNi_5 composite electrodes prepared from bare and Ni-P encapsulated particles

Table 1 Discharge capacity, exchange current density of $\text{H}_2\text{O}/\text{H}_2$ system, and corrosion kinetic parameters found on the basis of $\log(\text{capacity})$ —cycle number fade for the electrodes synthesized from bare and Ni-P encapsulated, LaNi_5 alloy (powder fraction: 20–50 μm , thickness of Ni-P coating: 1 μm , charge/discharge rate: $-186/+186 \text{ mA g}^{-1}$, 6 M KOH, Ar, 22 °C)

Parameter	Bare powder particles	Particles encapsulated
$Q_{0,\text{disch}} [\text{mA h g}^{-1}]$	186	190
$i_{\text{H}_2\text{O}/\text{H}_2}^0 [\text{mA g}^{-1}]$	39 ($N = 5$)	42 ($N = 5$)
	105 ($N = 20$)	121 ($N = 20$)
	131 ($N = 50$)	149 ($N = 50$)
	118 ($N = 90$)	155 ($N = 90$)
$k_{\text{degr}} [\text{cycle}^{-1}]$	$6.5 \cdot 10^{-3}$	$5.0 \cdot 10^{-3}$
$N_{1/2}$	106	139
$r_{\text{corr},0} [\text{g cm}^{-3} \text{ cycle}^{-1}]$	0.040	0.033

The exchange current densities of $\text{H}_2\text{O}/\text{H}_2$ system, calculated on the basis of potential jump (ΔE) [Eq. (4 and 5)] for the successive cycles and for bare and encapsulated electrode material, are shown in Fig. 4. Generally, up to $N \approx 60$, the exchange currents continuously increase with cycling and are over 15 % greater for the encapsulated material. However, for $N > 60$, there appears a clear tendency for $i_{\text{H}_2\text{O}/\text{H}_2}^0$ to fall down (for bare powder material) or to settle up (for encapsulated material). For encapsulated material, in spite of long-lasting cycling, $i_{\text{H}_2\text{O}/\text{H}_2}^0$ remains practically constant and equals approx. 155 mA g^{-1} . Similar $i_{\text{H}_2\text{O}/\text{H}_2}^0$ values have been found for Ni-P encapsulated $\text{LaNi}_{4.5}\text{Co}_{0.5}$ material [22]. The relatively large values of exchange currents for both kinds of encapsulated alloys can be attributed to the presence of metallic nickel on the particle surface. As it is known, nickel has documented catalytic properties towards the $\text{H}_2\text{O}/\text{H}_2$ system [32–34]. It is also worth mentioning that the electroless nickel coatings are in significant degree amorphous. It results from literature data [34] that amorphisation of nickel containing films favors increase of $i_{\text{H}_2\text{O}/\text{H}_2}^0$. To sum up, the modification of LaNi_5 storage alloy surface by electroless encapsulation of its particles with Ni-P coatings not only inhibits degradation of the active material with long-lasting cycling but improves its hydrogen charge/discharge kinetics as well.

All the parameters describing the functional properties of hydride electrodes prepared from uncoated- and encapsulated LaNi_5 powders are listed for comparison in Table 1.

Conclusions

1. After about 30 charge/discharge ($-186/+186 \text{ mA/g}$) cycles of LaNi_5 composite electrode exposure in 6 M KOH solution, the logarithm of discharge capacity linearly decreases with cycle number which satisfies the first

order reaction kinetics law. The slopes of obtained straight lines are measure of electrode material corrosion rate.

2. The LaNi_5 particle encapsulation with Ni-P increases the half capacity cycle number from 106 to 139
3. The encapsulation of active LaNi_5 material with 1 μm thick Ni-P coating inhibits the storage material corrosion process by over 20 %. Additionally, the exchange current densities of the $\text{H}_2\text{O}/\text{H}_2$ system on Ni-P covered particles are approx. 15 % greater than those on unmodified surface and, contrary to bare particles, do not exhibit any tendency to drop with long-lasting cycling

Acknowledgments The investigations have been supported by WIPiTM Statutory Research of Czestochowa Univ. Technology. The authors express their gratitude to professor Maria Sozanska for her help in SEM examinations.

Open Access This article is distributed under the terms of the Creative Commons Attribution 4.0 International License (<http://creativecommons.org/licenses/by/4.0/>), which permits unrestricted use, distribution, and reproduction in any medium, provided you give appropriate credit to the original author(s) and the source, provide a link to the Creative Commons license, and indicate if changes were made.

References

1. Young K, Nei J (2013) The current status of hydrogen storage alloy development for electrochemical applications. *Materials* 6:4574–4608
2. Tliha M, Khaldi C, Boussami S, Fenineche N, El-Kedim O, Mathlouthi H, Lamloumi J (2014) Kinetic and thermodynamic studies of hydrogen storage alloys as negative electrode materials for Ni/MH batteries: a review. *J Solid State Electrochem* 18:577–593
3. Liu Y, Pan H, Gao M, Wang Q (2011) Advanced hydrogen storage alloys for Ni/MH rechargeable batteries. *J Mater Chem* 21:4743–4755
4. Feng F, Geng M, Northwood DO (2001) Electrochemical behaviour of intermetallic-based metal hydrides used in Ni/metal hydride (MH) batteries: a review. *Int J Hydrog Energy* 26:725–734
5. Petrii OA, Levin EE (2007) Hydrogen-accumulating materials in electrochemical systems. *Russ J General Chem* 77:790–796
6. Zhao X, Ma L (2009) Recent progress in hydrogen storage alloys for nickel/metal hydride secondary batteries. *Int J Hydrog Energy* 34:4788–4796
7. Wang Q, Zhu D, Zhou W, Zhong C, Wu C, Chen Y (2016) High-temperature electrochemical performance of low-cost La–Ni–Fe based hydrogen storage alloys with different preparation methods. *Mater Research Bull* 76:28–36
8. Reilly JJ, Adzic GD, Johnson JR, Vogt T, Mukerjee S, McBreen J (1999) The correlation between composition and electrochemical properties of metal hydride electrodes. *J Alloys Compd* 293:295: 569–582
9. Durairajan A, Haran BS, White RE, Popov BN (2000) Pulverization and corrosion studies of bare and cobalt encapsulated metal hydride electrodes. *J Power Sources* 87:84–91
10. Durairajan A, Haran BS, Popov BN, White RE (1999) Cycle life and utilization studies on cobalt microencapsulated AB_5 type metal hydride. *J Power Sources* 83:114–120
11. Souza EC, Ticianelli EA (2003) Effect of partial substitution of nickel by tin, aluminum, manganese and palladium on the properties of LaNi_5 -type metal hydride alloys. *J Braz Chem Soc* 14:544–550
12. Notten PHL, Hokkelling P (1991) Double-phase hydride forming compounds: a new class of highly electrocatalytic materials. *J Electrochem Soc* 138:1877–1885
13. Ferey A, Cuevas F, Latroche M, Knosp B, Bernard P (2009) Elaboration and characterization of magnesium-substituted $\text{La}_3\text{Ni}_{19}$ hydride forming alloys as active materials for negative electrode in Ni-MH battery. *Electrochim Acta* 54:1710–1714
14. Belgacem YB, Khaldi C, Boussami S, Lamloumi J, Mathlouthi H (2014) Electrochemical properties of LaY_2Ni_9 hydrogen storage alloy used as an anode in nickel-metal hydride batteries. *J Solid State Electrochem* 18:2019–2026
15. Beck F, Ruetschi P (2000) Rechargeable batteries with aqueous electrolytes. *Electrochim Acta* 45:2467–2482
16. Dymek M, Bala H (2014) Hydrogen diffusivity in the massive LaNi_5 electrode using voltammetry technique. *J Solid State Electrochem* 18:3033–3037
17. Sakai T, Yuasa A, Ishikawa H, Miyamura H, Kuriyama N (1991) Nickel-metal hydride battery using microencapsulated alloys. *J Less-Common Met* 172–174:1194–1204
18. Wada M, Yoshinaga H, Kajita O, Sakai T, Irikawa M, Miyamura H, Kuriyama N, Uehara I (1993) Production of copper-alloy complex granules for nickel/metal hydride electrodes. *J Alloys Compd* 192: 164–166
19. Dymek M, Moscicki A, Sozanska M, Gesiarz K (2013) Electroless encapsulation of LaNi_5 powder particles with Ni-P protective layers. *Ochr przed Koroz* 56:505–507
20. Pratt AS, Willey DB, Harris IR (1999) High performance metal hydride alloy for rechargeable battery technology: platinum metals enhance alloy surface performance. *Platinum Metals Rev* 43:50–58
21. Purushothama BK, Wainright JS (2012) Analysis of pressure variations in a low-pressure nickel-hydrogen battery. Part 2: cells with metal hydride storage. *J Power Sources* 206:421–428
22. Bala H, Dymek M (2015) Corrosion degradation of powder composite hydride electrodes in conditions of long-lasting cycling. *Mater Chemistry Phys* 167:265–270
23. Dymek M, Bala H (2013) Effect of electrochemical cycling of LaNi_5 powder composite material on hydrogen diffusivity at pressures of 0.08–30 bar. *Ochr przed Koroz* 56:3–6
24. Dymek M, Bala H, Drulis H, Hackemer A (2015) Hydrogenation and corrosion properties of $\text{LaNi}_{4.5}\text{Co}_{0.5}$ -based alloy doped with 1.7 at% Sn. *Solid State Phenom* 227:263–266
25. Rożdżyńska-Kiełbik B, Iwasieczko W, Drulis H, Pavlyuk VV, Bala H (2000) Hydrogen equilibria characteristics of $\text{LaNi}_{5-x}\text{Zn}_x$ intermetallics. *J Alloys Compd* 298:237–243
26. Dymek M, Bala H (2013) Progress in evaluation of metal hydride electrode charge time and time of oxide phases reduction. *Ochr przed Koroz* 56:115–119
27. Dymek M, Moscicki A, Bala H (2013) Peculiarities of LaNi_5 -powder/PVDF bonded composite/alkaline electrolyte interaction at repeating charge/discharge cycles. *Ochr przed Koroz* 56:502–505
28. Bala H, Giza K, Kukula I (2010) Determination of hydrogenation ability and exchange current of $\text{H}_2\text{O}/\text{H}_2$ system on hydrogen absorbing metal alloys. *J Appl Electrochem* 40:791–797
29. Bala H, Dymek M, Adamczyk L, Giza K, Drulis H (2014) Hydrogen diffusivity, kinetics of $\text{H}_2\text{O}/\text{H}_2$ charge transfer and corrosion properties of LaNi_5 powder, composite electrodes in 6 M KOH solution. *J Solid State Electrochem* 18:3039–3048
30. Bala H, Kukula I, Giza K, Marciniak B, Rozycka-Sokolowska E, Drulis H (2012) Evaluation of the electrochemical hydrogenation and corrosion behaviour of LaNi_5 -based materials using galvanostatic charge/discharge measurements. *Int J Hydrog Energy* 37:16817–16822

31. Dymek M, Bala H, Hackemer A, Drulis H (2015) Electrochemical hydrogenation and corrosion properties of $\text{LaNi}_{4.5}\text{Co}_{0.5}$ alloy doped with aluminum. *Solid State Ionics* 271:116–120
32. Endoh E, Otuma H, Morimoto T, Oda Y (1987) New Raney nickel composite-coated electrode for hydrogen evolution. *Int J Hydrog Energy* 12:473–479
33. Hu WK, Shen PW, Zhang YS, Wang GS, Song DY, Zhou ZX (1995) Application of ion beam sputtering to electrocatalysts of hydrogen storage alloy. *Int J Hydrog Energy* 20:245–246
34. Ezaki H, Morinaga M, Watanabe S (1993) Hydrogen overpotential for transition metals and alloys and its interpretation using an electronic model. *Electrochim Acta* 38:557–564